Heliyon

Received:
4 May 2018
Accepted:
28 June 2018

Cite as: Mohun Ramratnam, Barrett Kenny, John W. Kyle, Brandi Wiedmeyer, Timothy A. Hacker, David Y. Barefield, Elizabeth M. McNally, Jonathan C. Makielski. Transgenic overexpression of the SUR2A-55 splice variant in mouse heart reduces infract size and promotes protective mitochondrial function. Heliyon 4 (2018) e00677. doi: 10.1016/j.heliyon.2018.e00677

Transgenic overexpression of the SUR2A-55 splice variant in mouse heart reduces infract size and promotes protective mitochondrial function

Mohun Ramratnam [a,b,*], **Barrett Kenny** [a], **John W. Kyle** [a], **Brandi Wiedmeyer** [a], **Timothy A. Hacker** [c], **David Y. Barefield** [d], **Elizabeth M. McNally** [d], **Jonathan C. Makielski** [a]

[a] *Division of Cardiovascular Medicine, Department of Medicine, University of Wisconsin School of Medicine and Public Health, Madison, WI, United States*

[b] *Cardiology Section, Medical Service, William. S. Middleton Memorial Veterans Hospital, Madison, WI, United States*

[c] *Cardiovascular Research Center, University of Wisconsin School of Medicine and Public Health, Madison, WI, United States*

[d] *Center for Genetic Medicine, Northwestern University, Chicago, IL, United States*

[*] Corresponding author.
E-mail address: mramrat@medicine.wisc.edu (M. Ramratnam).

Abstract

ATP-sensitive potassium channels found in both the sarcolemma (sarcK_{ATP}) and mitochondria (mitoK_{ATP}) of cardiomyocytes are important mediators of cardioprotection during ischemic heart disease. Sulfonylurea receptor isoforms (SUR2), encoded by *Abcc9*, an ATP-binding cassette family member, form regulatory subunits of the sarcK_{ATP} channel and are also thought to regulate mitoK_{ATP} channel activity. A short-form splice variant of SUR2 (SUR2A-55) was previously shown to target mitochondria and display diaxoxide and ATP insensitive K_{ATP} activity when co-expressed with the inward rectifier channels Kir6.2 and Kir6.1. We hypothesized that mice with cardiac specific overexpression of SUR2A-55 would mediate cardioprotection from ischemia by

https://doi.org/10.1016/j.heliyon.2018.e00677

altering mitoK$_{ATP}$ properties. Mice overexpressing SUR2A-55 (TG$^{SUR2A-55}$) in cardiomyocytes were generated and showed no significant difference in echocardiographic measured chamber dimension, percent fractional shortening, heart to body weight ratio, or gross histologic features compared to normal mice at 11−14 weeks of age. TG$^{SUR2A-55}$ had improved hemodynamic functional recovery and smaller infarct size after ischemia reperfusion injury compared to WT mice in an isolated hanging heart model. The mitochondrial membrane potential of TG$^{SUR2A-55}$ mice was less sensitive to ATP, diazoxide, and Ca^{2+} loading. These data suggest that the SUR2A-55 splice variant favorably affects mitochondrial function leading to cardioprotection. These data support a role for the regulation of mitoK$_{ATP}$ activity by SUR2A-55.

Keywords: Medicine, Cardiology, Physiology

1. Introduction

Myocardial ATP-sensitive potassium channels (K$_{ATP}$) were first described more than 30 years ago [1] and are major contributors to pre-conditioning and cardioprotection [2, 3, 4]. They were first identified in the sarcolemma (sarcK$_{ATP}$) but soon after K$_{ATP}$ channels were also reported in the inner membrane of mitochondria (mitoK$_{ATP}$) [5]. These channels are closed under normal physiologic conditions but open in response to acute stress leading to changes in cytoplasmic and mitochondrial function that promote cardioprotection [6, 7, 8].

The molecular composition of sarcK$_{ATP}$ has been identified as a hetero-octomer of four Kir6.x (Kir6.1 or Kir 6.2) pore forming subunits and four sulfonylurea receptor (SUR1 or SUR2) regulatory subunits from the ABC binding cassette family of membrane proteins [9]. In addition, both splice variants of the SUR2 gene (SUR2A and SUR2B) form functional sarcK$_{ATP}$ [10]. Different tissues display different subunit expression, giving rise to functionally distinct sarcK$_{ATP}$ [11, 12, 13]. The cardiac ventricular sarcK$_{ATP}$ is composed of SUR2A and Kir6.2 [14]. While there is a large body of literature studying the constituents of ventricular sarcK$_{ATP}$, the molecular makeup of mitoK$_{ATP}$ in the heart has been more elusive. The most recent candidate for the pore forming subunit of mitoK$_{ATP}$ is the renal outer medullary potassium channel (ROMK or Kir1.1) which was first supported using a proteomic analysis of the mitochondrial inner membrane [15, 16]. In addition, evidence exists that SUR2 gene products exist in mitochondria and play a role in mitoK$_{ATP}$ channel activity [17, 18, 19].

We described a 55 kDa splice variant (SUR2A-55) formed by intra-exonic splicing that is located predominantly in mitochondria [20] which other labs have also identified [21]. K$_{ATP}$ activity was recorded when SUR2A-55 was targeted to the sarcolemma by deleting a mitochondrial targeting sequence and when co-expressed with

https://doi.org/10.1016/j.heliyon.2018.e00677

Kir6.2 and Kir6.1 in heterologous cells [20, 22]. We also found that mice engineered with targeted disruption of exon 14−18 of SUR2 ($SUR2^{-/-}$) lacked full-length SUR2 but unexpectedly exhibited cardioprotection from ischemia reperfusion (IR) injury despite the absence of pinacidil, diazoxide, or glybenclamide sensitive sarcK_{ATP} currents [23, 24, 25]. The gene product that encodes the SUR2A-55 splice variant was not perturbed by the deletion used to generate $SUR2^{-/-}$ mice, and correspondingly mitochondria from these mice had favorable mitochondrial bioenergetics characterized by slight mitochondrial membrane depolarization at rest, insensitivity to ATP and diazoxide, increased reactive oxygen species (ROS), and tolerance to Ca^{2+} loading [26]. Furthermore, K_{ATP} currents in heterologous systems produced by co-expression of SUR2A-55 and Kir were less sensitive to block by ATP, more resistant to intracellular Ca^{2+}, and less sensitive to K_{ATP} drugs [22] compared to full-length SUR2A. Recently, a second SUR2 knockout mouse was created by removing exon 5, an exon found in both SUR2 and SUR2A-55. This mutation produced early lethality and failure to transition from fetal to adult myocardial metabolism [27]. These mice, unlike the prior $SUR2^{-/-}$ mice, lacked both full-length SUR2 and the SUR2A-55 splice variant. From these mouse studies, we hypothesized that the SUR2A-55 splice variant plays an important role in mitochondrial function and cardioprotection.

To further understand the physiologic implication of SUR2A-55 we present here an investigation of novel mice overexpressing the SUR2A-55 splice variant in cardiac tissue, which we refer to as $TG^{SUR2A-55}$.

2. Materials and methods

2.1. Construction of a cardiomyocyte-specific SUR2A-55 overexpressing mouse ($TG^{SUR2A-55}$)

Transgenic mice expressing SUR2A-55 were generated in the University of Wisconsin Transgenic Animal facility. The 1.5 kb cDNA for SUR2A-55 bracketed by Xho I sites was cut with and ligated into the Sal I cloning site downstream of the 5.5 kb α-myosin heavy chain (α-MHC) cardiac-specific promoter and upstream from the 0.6 kb human growth hormone poly A [28]. The α-MHC-SUR2A-55 construct was linearized with Sac II and gel purified and injected into the male pronucleus of FVB single-cell mouse embryos and implanted into psuedopregnant females. Offspring were screened by Southern blotting of genomic DNA using a 0.7 kb probe corresponding to the first 0.7 kb of the SUR2A-55 cDNA. Chimeric mice were bred with FVB mice and colonies were maintained by breeding hemizygous transgenic mice with WT FVB mice in accordance with the standards set by the Animal Care and Use Committees at the University of Wisconsin. All animal experiments were performed in compliance with relevant laws and institutional guidelines and

https://doi.org/10.1016/j.heliyon.2018.e00677

approved by the local animal ethics committee of the University of Wisconsin. Male mice were selected for study owing to evidence of sex differences in myocardial protection [29, 30]. Sex differences are likely to be important and will be the subject of additional study.

2.2. RNA analysis

Total RNA was extracted from mouse ventricle using TRIzol reagent (Invitrogen ThermoFisher, Waltham, MA) according to the manufacturer's instructions. First-strand cDNA was synthesized from 3 μg of total RNA using the SuperScript III First-Strand Synthesis System for RT-PCR (Invitrogen ThermoFisher, Waltham, MA). The quantitative real-time PCR (qPCR) reaction was performed using a 1:2 dilution of cDNA in a total of 20 μL with 10 μL Gene Expression Master Mix (Integrated DNA Technologies, Coralville, IA) and a final concentration of 500 nM forward primer, 500 nM reverse primer, and 250 nM probe. Each cDNA sample analyzed for gene expression by qPCR using the BioRad CFX 96 Real-Time PCR Detection System. Amplification data were analyzed using the delta-delta Cq method with the relative standard curve method to obtain reaction efficiencies of 90−105%. The conditions of qPCR for all primer/probe sets were as follows: an initial denaturation at 95 °C for 3 min followed by 40 cycles at 95 °C for 15 s and 52 °C for 1 min. Oligonucleotide primers were designed using published sequence data from GenBank with the aid of PrimeQuest Design Tool (Integrated DNA Technologies, Coralville, IA). The primer and hydrolysis probe sequences used are shown in Table 1. The mRNA expression was normalized to the levels of *Actb* and *Gapdh* mRNA as the reference genes.

Table 1. Primers used to detect K_{ATP} channel subunits (SUR2-55 and SUR2) and reference genes in qPCR studies.

Encoding protein name	Gene name	Reference sequence IDs	Primer and probe sequences (5′-3′)
SUR2-55	*Abcc9*	DQ991969 DQ991970	F-TGTACTGGGTAATGGCCTTTATTA R-TGGAGGCTGTCAGAACAATG PRB-/56-FAM/AGATAGTCC/ZEN/ GTCCTGACCTCCCAC/3IABkFQ/
SUR2	*Abcc9*	D86037.2 D86038.2	F-CCACCACAACCTCCTCAATAA R-TGGTCGATGATGTTCGTATCAG PRB-/5HEX/AGGTTCTTT/ZEN/ GATACCACACCGCTGG/3IABkFQ/
ACTB	*Actb*	NM_007393.5	F-GATTACTGCTCTGGCTCCTAG R-GACTCATCGTACTCCTGCTTG PRB-/56-FAM/CTGGCCTCA/ZEN/ CTGTCCACCTTCC/3IABkFQ/
GAPDH	*Gapdh*	NM_008084.3	F-AATGGTGAAGGTCGGTGTG R-GTGGAGTCATACTGGAACATGTAG PRB-/56-FAM/TGCAAATGG/ZEN/ CAGCCCTGGTG/3IABkFQ/

https://doi.org/10.1016/j.heliyon.2018.e00677

2.3. Western blot analysis

Total protein was isolated from mouse ventricle. Ventricle tissue was solubilized in RIPA buffer (150 mM NaCl, 1% NP40, 0.5% sodium deoxycholate, 0.1% SDS, Tris, pH 7.5; Pierce, Rockford, IL) with added protease inhibitors and phenylmethylsulfonyl fluoride. All samples were sonicated 3 times, 10 seconds each at an amplitude of 60% and incubated at 4 °C for 2 hours. Protein concentrations were determined using the BCA method. Tissue and whole cell lysates were fractionated on 4−12% Bis-Tris SDS-PAGE gradient gel (Invitrogen ThermoFisher, Waltham, MA) and transferred to a polyvinylidene difluoride membrane using a transfer apparatus according to the manufacturer's protocols (Invitrogen ThermoFisher, Waltham, MA). After blocking by incubation with 5% nonfat milk in PBST (137 mM NaCl, 10 mM Na_2HPO_4, 1.8 mM KH2PO_4, 2.7 mM KCl, 0.1% (v/v) Tween 20, pH 7.4) for 60 min, the membrane was washed with PBST and incubated with antibodies at 4 °C overnight on a rocker. Immunoblots were performed with SUR2 specific antibodies that were generated as previously described [31] (1:500 dilution). Membranes were washed five times PBST for 5 min each and incubated with a 1:10,000 dilution of horseradish peroxidase-conjugated anti-rabbit antibodies for 1 h at room temperature on a rocker. Blots were washed with PBST five times and developed with the ECL system (Pierce, Rockford, IL) according to the manufacturer's protocols.

2.4. Echocardiography

Transthoracic echocardiography was performed on 11−14 week old mice after sedation with 3% isoflurane using a VisualSonics Vevo 770 machine with a 30-MHz transducer [18]. Left ventricular end diastolic (LVEDD), left ventricular end systolic (LVESD), anterior wall thickness in diastole (LVAW;d) and posterior wall thickness in diastole (LVPW;d) were obtained from M-mode tracings. LV fractional shortening was calculated as (LVEDD−LVESD)/LVEDD×100%.

2.5. Histopathology

Twelve week old $TG^{SUR2A\text{-}55}$ and WT mice hearts were sectioned and stained with hematoxylin and eosin to assess myofiber architecture and Masson's trichrome to assess interstitial fibrosis.

2.6. Langendorff ischemia reperfusion experiments

Mice were anesthetized with inhaled 3% isoflurane and then euthanized by cervical dislocation. Hearts were rapidly excised and placed in chilled heparinized modified Krebs-Henseleit buffer (KHB) (118 mM NaCl, 4.7 mM KCl, 1.2 mM $MgSO_4$, 1.2 mM KH_2PO_4, 25 mM $NaHCO_3$, 2.5 mM $CaCl_2$, 0.5 mM EDTA, 5 mM glucose,

https://doi.org/10.1016/j.heliyon.2018.e00677

and 5 mM sodium pyruvate). Extra-cardiac tissue was dissected and discarded while the aorta was located. The aorta was then cannulated with the use of a 22 gauge cannula. The cannula was secured in place with a 6.0 silk suture. Hearts were then perfused at a constant pressure of 80 mmHg on a custom made Langendorff apparatus with the modified KHB and equilibrated with 95% O_2 and 5% CO_2 at 37 °C. The left auricle was then excised and a fluid filled balloon catheter constructed from a commercially available kit (Harvard Apparatus, Holliston, MA) was placed in the left ventricle. The balloon catheter was attached to a APT300 pressure transducer (Harvard Apparatus, Holliston, MA) and baseline left ventricular pressure was set between 5-10 mm Hg. Baseline cardiac function was recorded for 30 minutes followed by 45 minutes of ischemia and then 60 minutes of reperfusion. Hearts were paced at 360 bpm via epicardial pacing leads with a Grass SD9 stimulator. Left ventricular pressure was recorded throughout the experimental protocol and analyzed using LabChart Pro (ADInstruments, Colorado Springs, CO). Hemodynamic variables are presented as % recovery to baseline values. Upon completion of reperfusion, hearts were rapidly removed from the Langendorff apparatus and perfused with 30 mM of KCl solution to arrest the hearts in diastole. Then the hearts were stained with 1% tetrazolium chloride solution for 10 minutes. The hearts were then sectioned into 7−8 slices. The sections were placed in 10% formalin and photographed the following day for the quantification of infarct size.

2.7. Isolation of mitochondria

Mitochondria from murine ventricular cardiac tissue were isolated by homogenization and differential centrifugation as previously described [26, 32]. Briefly, hearts were quickly excised after thoracotomy and placed in ice-cold isolation buffer (50 mM sucrose, 200 mM mannitol, 5 mM KH_2PO_4, 1 mM EGTA, and 5 mM 3-(N-morpholino)propanesulfonic acid). Hearts were manually minced, digested for 10 minutes with 0.1 mg/ml of trypsin and mitochondria were isolated with differential centrifugation. The final mitochondrial pellet was resuspended in ice cold isolation buffer with 0.1% bovine serum albumin. Protein concentrations were determined and 0.5 mg of mitochondria were used to perform each mitochondrial experimental run. Total isolation time was <2 hours and mitochondria were used within 1−2 hours of isolation.

2.8. Mitochondrial membrane potential and tolerance to Ca^{2+}

Mitochondrial membrane potential ($\Delta\psi_m$) was monitored spectrophotometrically as previously described [26]. Briefly, with the use of rhodamine 123 (5 nM) and excitation λ_{ex} of 503-nm and emission λ_{em} of 527-nm, 0.5 mg of mitochondria were added to a cuvette containing malate (5 mM), pyruvate (5 nM) and oligomycin (5 μM). $\Delta\psi_m$ was assessed in the presence of high (500 μM) and low (10 μM) ATP concentrations

https://doi.org/10.1016/j.heliyon.2018.e00677

as well as the addition of diazoxide (0.1 mM) where indicated. The ionophore carbonylcyanide-4-trifluoromethoxyphenylhydrazone (FCCP; 1 μM) was used to depolarize the mitochondrial membrane at the end of each experiment. The $\Delta\psi_m$ is expressed as the difference in measured rhodamine 123 fluorescence between the FCCP induced maximum and a stable baseline after mitochondrial addition represented as rhodamine 123 arbitrary florescense units (afu). The $\Delta\psi_m$ response to diazoixde is represented as the change in rhodamine 123 florescense after a stable baseline is achieved from the addition of mitochondria. Tolerance to Ca^{2+} of the $\Delta\psi_m$ was assessed as previously described [26]. Briefly, in the presence of 200 μM of ATP and EGTA-free buffer, 20-μM increments of Ca^{2+} were added and $\Delta\psi_m$ was monitored until total Ca^{2+} concentration reached 140 μM. The membrane potential uncoupler carbonylcyanide-4-trifluoromethoxyphenylhydrazone (FCCP; 1 μM) was used at the end of each experimental run and $\Delta\psi_m$ was analyzed relative to the fluorescence after the addition of FCCP. The cumulative amount of Ca2+ needed to depolarize the $\Delta\psi_m$ by 20% was determined.

2.9. Statistical analysis

Data are reported as mean ± standard error. Statistical analysis were performed using the R program 3.4.2 (R Foundation for Statistical Computing) and Microsoft Excel (Microsoft, Redmond, WA) with a P value < 0.05 considered significant. Comparison between 2 groups were made using the two-tailed Student's t-test. Ischemia-reperfusion experiments of Langendorff-perfused hearts were subjected to two-way ANOVA for comparison between groups.

3. Results

3.1. Overexpression of SUR2A-55 in $TG^{SUR2A-55}$ mice

Hearts from 10-14 week old mice were used for mRNA and protein analysis. Hearts from $TG^{SUR2A-55}$ mice showed similar expression of full-length SUR2A mRNA but significantly increased SUR2A-55 mRNA compared to littermate WT mice (Fig. 1B). Qualitatively, the protein expression of SUR2A in the transgenic mice was not changed but there was increased protein expression of SUR2A-55 in $TG^{SUR2A-55}$ mice compared to WT mice (Fig. 1C). While previous reports have detected SUR2A-55 in WT mouse hearts [20] and cardiomyoctyes [21], in our current FVB mouse line the level of SUR2A-55 was below the level of detection of western blotting and qPCR.

3.2. Cardiac structure and function in $TG^{SUR2A-55}$ mice

Wall thickness and chamber dimensions were not significantly different between WT and $TG^{SUR2A-55}$ mice during baseline echocardiography (Fig. 2). Heart rates

https://doi.org/10.1016/j.heliyon.2018.e00677

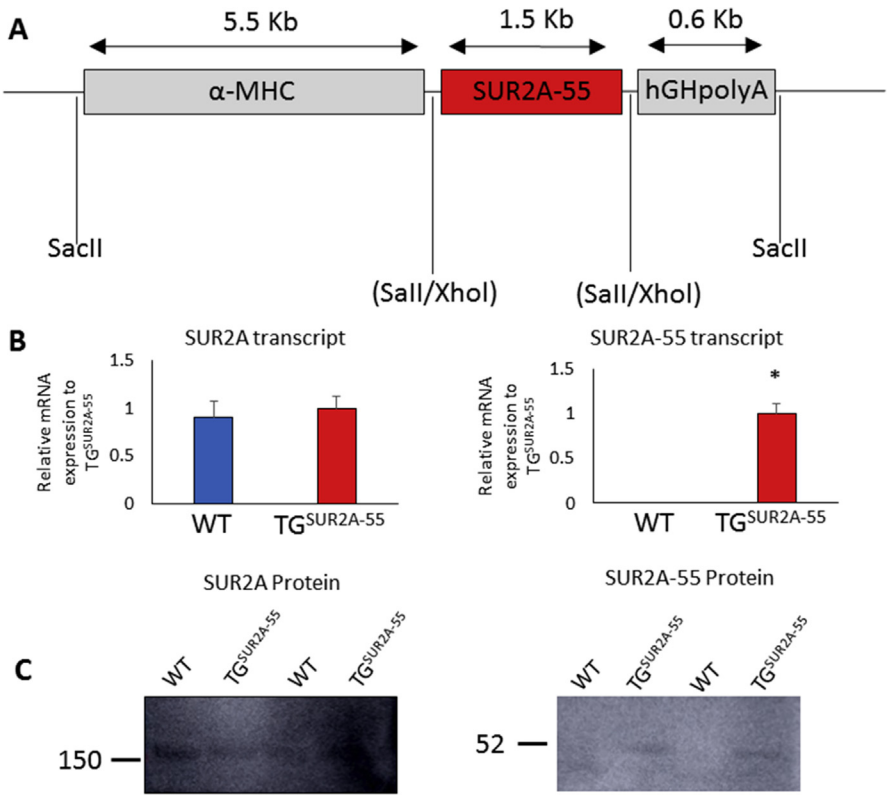

Fig. 1. Construction of a cardiomyocyte specific SUR2A-55 overexpressing mouse. (A) Organization of the α-MHC-SUR2A-55 construct. (B) Relative total cardiac SUR2A and SUR2A-55 mRNA expression determined by qPCR and (C) protein expression. N = 3/group for qPCR, $*P < 0.001$. Full images of western blots are presented in supplementary Fig. 1.

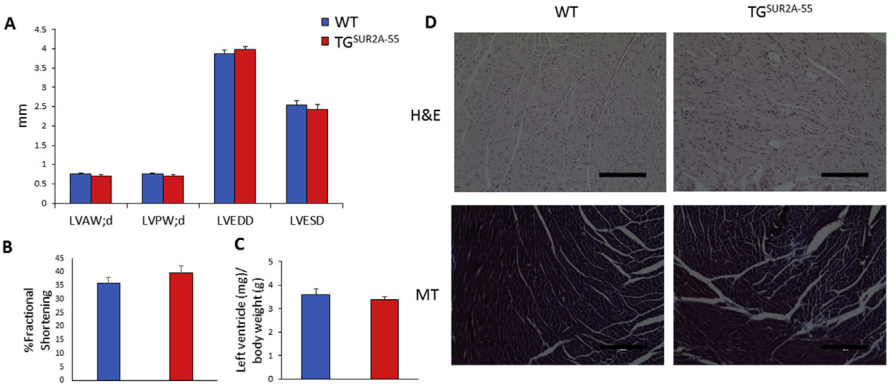

Fig. 2. Echocardiography and histology for WT and TG$^{SUR2A-55}$ mice. There were no significant difference in echocardiographic chamber dimensions and % fractional shortening between WT and TG$^{SUR2A-55}$ mice (A, B). The heart to body weight ratio was also not significantly different between WT and TG$^{SUR2A-55}$ mice (C). There were no gross changes seen in histology between WT and TG$^{SUR2A-55}$ mice (D). N = 12 for WT mice and N = 13 for TG$^{SUR2A-55}$ mice in A,B and C. LVAW;d, left ventricular anterior wall in diastole; LVPW;d, left ventricular posterior wall in diastole; LVEDD, left ventricular end diastolic dimension; LVESD, left ventricular end systolic dimension; H&E, Hematoxylin Eosin; MT, Mason trichrome. (D) Bar = 200 μm.

https://doi.org/10.1016/j.heliyon.2018.e00677

were not significantly different between WT and $TG^{SUR2A-55}$ mice (470 bpm ± 66 vs. 461 bpm ± 61). Left ventricular mass to body weight ratio was not significantly different between WT and $TG^{SUR2A-55}$ mice (3.58 ± 0.25 vs. 3.37 ± 0.12, respectively). Baseline *ex vivo* hemodynamic characteristics showed a reduction in +dp/dt and −dp/dt in $TG^{SUR2A-55}$ mice compared to WT mice (Fig. 3A) but *in vivo* assessment of % fractional shortening (35 ± 2 vs. 40 ± 3, respectively) did not show any significant difference (Fig. 2). There were no gross histologic differences seen between WT and $TG^{SUR2A-55}$ mice with hematoxylin and eosin staining (Fig. 2). Trichrome staining did not show any gross differences in cardiac fibrosis.

3.3. $TG^{SUR2A-55}$ mice are protected against ischemia-reperfusion injury

Isolated hearts from $TG^{SUR2A-55}$ and WT mice were subjected to 45 minutes of no flow ischemia and then 60 minutes of reperfusion. Baseline hemodynamic characteristics are shown in Table 2 and subsequent hemodynamic variables are presented as % recovery to baseline values (Fig. A−C). $TG^{SUR2A-55}$ mice had improved left ventricular developed pressure (LVDP) compared to WT mice during reperfusion ($P < 0.0001$ by two-way ANOVA, Fig. 3A). $TG^{SUR2A-55}$ mice also had improved +dp/dt and −dp/dt compared to WT mice during reperfusion ($P < 0.0001$ by two-way ANOVA, Fig. 3B and C). Representative heart sections stained with 1% TTC from $TG^{SUR2A-55}$ and WT mice after IR injury (Fig. 4A) showed significantly reduced myocardial infarction in $TG^{SUR2A-55}$ compared to WT mice (Fig. 4B).

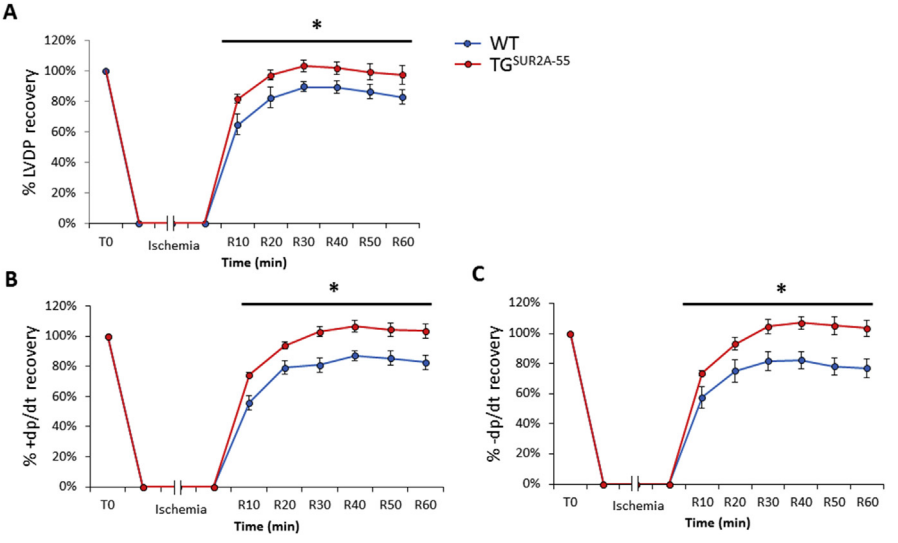

Fig. 3. The effect of global ischemia on cardiac hemodynamic function in WT vs. $TG^{SUR2A-55}$ mice. After IR injury, $TG^{SUR2A-55}$ mice have improved functional recovery compared to WT mice in respect to the % recovery of baseline LV developed pressure (A), +dp/dt (B) and −dp/dt (C). N = 7/group. *$P <$ 0.05 for two-way ANOVA.

https://doi.org/10.1016/j.heliyon.2018.e00677

Table 2. Baseline hemodynamic characteristics of isolated perfused hearts.

	WT	$TG^{SUR2A-55}$	P value
LVDP (mmHg)	89.2 ± 15.1	77 ± 10.9	0.067
EDP (mmHg)	8.4 ± 3.7	8.9 ± 4.3	0.41
+dp/dt (mmHg/s)	2958 ± 378	2471 ± 488	0.03
−dp/dt (mmHg/s)	−1836 ± 234	−1435 ± 232	0.003

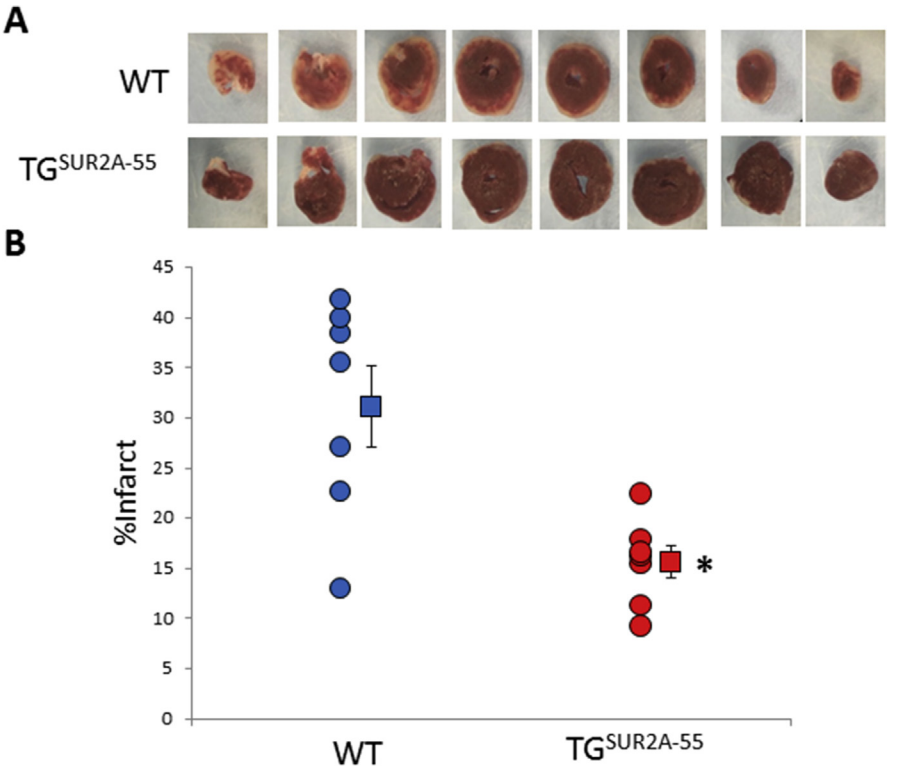

Fig. 4. The effect of global ischemia on infarct size in WT vs. $TG^{SUR2A-55}$ mice. (A) Representative sections after IR injury from WT and $TG^{SUR2A-55}$ mice. (B) $TG^{SUR2A-55}$ mice have significantly less infarct size compared to WT littermate controls after IR injury. Circles represent individual data points. Squares represent mean values. N = 7/group. *$P < 0.01$.

3.4. The $\Delta\psi_m$ of $TG^{SUR2A-55}$ mice are less sensitive to ATP and diazoxide

The mitochondrial membrane potential ($\Delta\psi_m$) was measured at low (10 μM) and high (500 μM) ATP concentrations in isolated mitochondria from $TG^{SUR2A-55}$ and WT mice with the substrates malate and pyruvate. Representative traces show that the sensitivity of $\Delta\psi_m$ to ATP was diminished in $TG^{SUR2A-55}$ mitochondria compared to WT mitochondria (Fig. 5A and B). There was a significant 14% difference in $\Delta\psi_m$ for WT mitochondria measured at low ATP vs. high ATP concentrations (90.1 ± 6.7 afu vs. 104.7 ± 1.6 afu, $P < 0.05$), while there was only a 4% difference

https://doi.org/10.1016/j.heliyon.2018.e00677

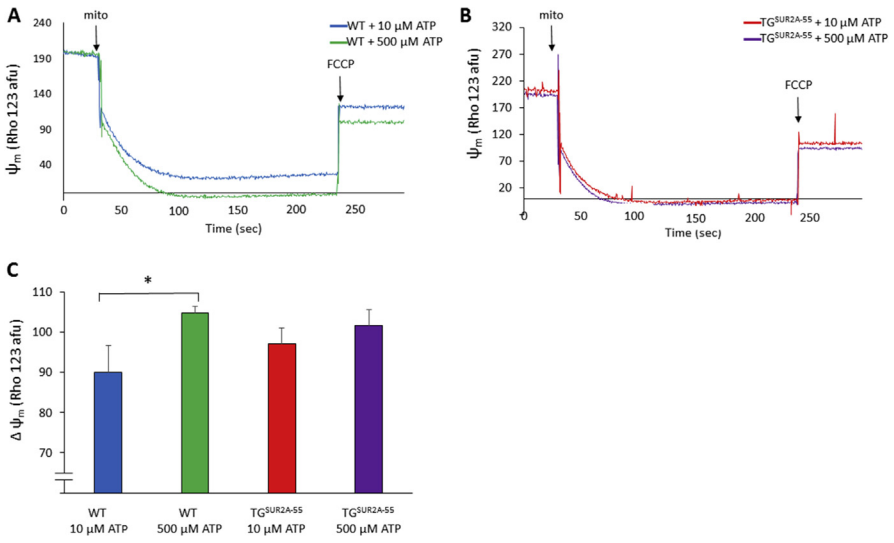

Fig. 5. ATP sensitivity of mitochondrial membrane potential (ψ_m) from WT and $TG^{SUR2A-55}$ mice mitochondria. (A) and (B) show measurements of ψ_m using rhodamine 123 fluorescence in isolated mitochondria from WT and $TG^{SUR2A-55}$ mouse hearts at 10 μM [ATP] and 500 μM [ATP]. (C) Summary data of $\Delta\psi_m$ (FCCP induced maxium − resting mitochondrial fluorescence) using high and low concentrations of ATP in WT and $TG^{SUR2A-55}$ mice. N = 6/group for experiments performed with 10 μM [ATP]; N = 4/group for experiments performed with 500 μM [ATP]. *$P < 0.05$.

in $\Delta\psi_m$ for $TG^{SUR2A-55}$ mitochondria measured at low vs. high ATP concentrations (97 ± 8.9 afu vs. 101 ± 8 afu, $P = 0.22$). Previous studies of $SUR2^{-/-}$ mice mitochondria found a significantly more polarized $\Delta\psi_m$ at high ATP concentrations compared to WT mice mitochondria [26]. However our current study did not find such a difference. In the presence of ATP, diazoxide decreased the $\Delta\psi_m$ in WT mitochondria more than the $\Delta\psi_m$ of $TG^{SUR2A-55}$ mitochondria (Fig. 6A). Cumulative experiments showed that WT mitochondria had a significantly greater response to diazoxide compared to $TG^{SUR2A-55}$ mice ($18\% \pm 0.02$ vs. $8\% \pm 0.02$, $P < 0.05$, Fig. 6B).

3.5. The $\Delta\psi_m$ of $TG^{SUR2A-55}$ mitochondria are more tolerant to Ca^{2+}

To test $\Delta\psi_m$ resistance to Ca^{2+}, $TG^{SUR2A-55}$ and WT mitochondria were challenged with 20 μM pulses of Ca^{2+} while $\Delta\psi_m$ was measured. Representative plots (Fig. 7A) show that WT mitochondria start to depolarize sooner and less Ca^{2+} is needed to depolarize mitochondria from WT compared to $TG^{SUR2A-55}$ hearts. ($P < 0.05$, Fig. 7B).

4. Discussion

In this investigation we studied whether the cardiomyocyte specific overexpression of the SUR2A-55 splice variant affects the response to myocardial IR injury and

https://doi.org/10.1016/j.heliyon.2018.e00677

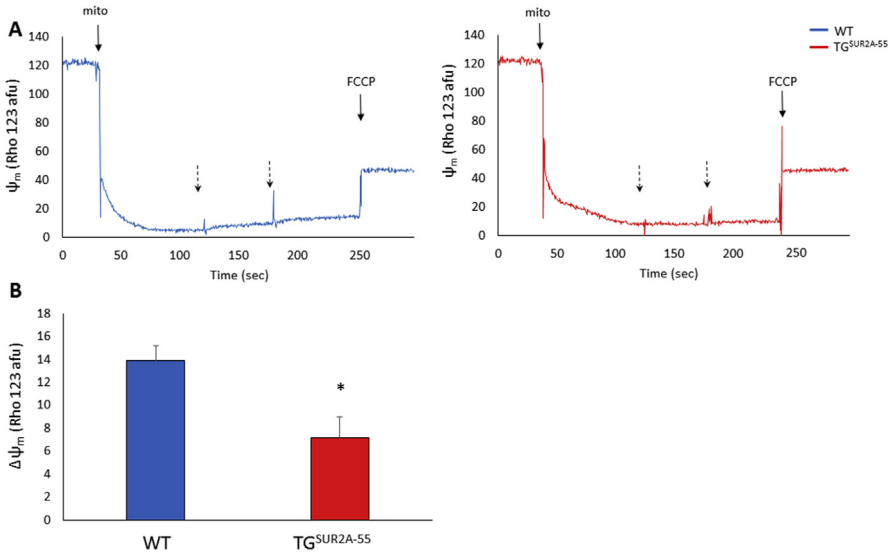

Fig. 6. Sensitivity of ψ_m to diazoxide in WT and $TG^{SUR2A-55}$ mice mitochondria. Representative measurements (A) of ψ_m using rhodamine 123 fluorescence showing a reduction in $TG^{SUR2A-55}$ mitochondria's response to additions of diazoxide (indicted by broken arrows) relative to WT mitochondria. (B) Summary data showing a greater change in ψ_m in WT mitochondria compared to $TG^{SUR2A-55}$ mitochondria to diazoxide. N = 4/group; $*P < 0.05$.

alters mitoK_{ATP} pharmacology. We found that at baseline there was no significant difference in echocardiographic parameters and gross histology between $TG^{SUR2A-55}$ and littermate WT control mice. $TG^{SUR2A-55}$ mice had improved infarct size and hemodynamic response when subjected to IR injury compared to WT mice. We further assessed isolated mitochondria from $TG^{SUR2A-55}$ mice to see if they have a bioenergentic profile consistent with a protected phenotype [26, 33]. The $\Delta\psi_m$ in $TG^{SUR2A-55}$ mitochondria were less responsive to ATP and diazoxide and exhibited an increased tolerance to Ca^{2+} loading compared to the $\Delta\psi_m$ in mitochondria from WT mice. K_{ATP} channels composed of SUR2A-55 subunits have reduced sensitivity to ATP and diazoxide [22], which is predicted since alternative mRNA splicing removes putative ATP binding sites. These results show that overexpression of SUR2A-55 leads to preserved resting *in vivo* cardiac structure and function while promoting cardioprotection from myocardial stress associated with a favorable mitochondrial phenotype.

4.1. SUR2A-55 overexpression leads to a viable phenotype

While we were unable to identity significant amounts of SUR2A-55 in resting WT hearts, prior studies have shown the presence of SUR2A-55 in mouse heart and localization to the mitochondria [20, 27]. In our study we found that baseline echocardiography-derived cardiac chamber size and function as well as heart to body weight ratio of $TG^{SUR2A-55}$ mice compared to WT mice were not significantly

https://doi.org/10.1016/j.heliyon.2018.e00677

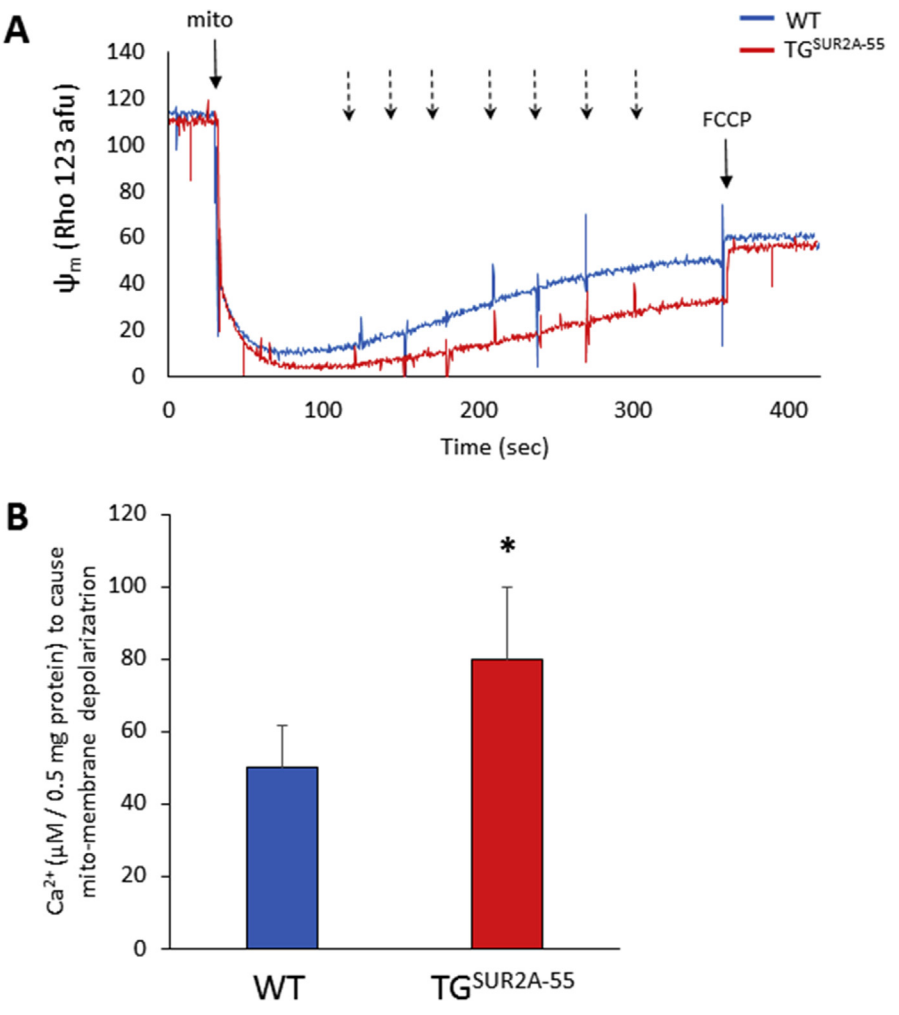

Fig. 7. Mitochondrial tolerance to Ca^{2+} overload. After addition of mitochondria and stabilization of florescence, 20 μM additions of Ca^{2+} (indicted by broken arrows) were given to the mitochondrial preparation as shown in A. The cumulative amount of calcium needed to depolarize the ψ_m at least 20% was quatified and shown in B among WT and $TG^{SUR2A-55}$ heart mitochondria. N = 4/group; $^*P < 0.05$.

different. We did, however, notice that in the Langendorff experiments, baseline +dp/dt and −dp/dt values were significantly less in the $TG^{SUR2A-55}$ compared to WT mice. The mechanism of the isolated heart baseline differences are unclear. It may be that $TG^{SUR2A-55}$ mice are more susceptible to cardiac depression when *ex vivo* or that the mitochondrial changes observed translate to subtle changes in cardiac performance when measured *ex vivo* compared to *in vivo*. In addition, $TG^{SUR2A-55}$ may be more sensitive to cardiac depression with the dose of anesthesia used for cervical dislocation. While the current overexpression model of SUR2A-55 leads to a viable mouse phenotype, recent data has suggested that deletion of all SUR2 products including the long-form and SUR2A-55 splice variant lead to lethality with a failure to transition from neonatal to mature adult metabolism [27]. Therefore, it is likely that the SUR2A-55 splice variant carries not only an important role in cardioprotection in

https://doi.org/10.1016/j.heliyon.2018.e00677

adulthood but also in development during the neonatal period. Transgenic mice that conserve the SUR2A-55 variant but do not have the long-form SUR2 due to deletion of exons 14−18 are viable and live to adulthood [34]. While studying substrate utilization and cardiac metabolism were outside the scope of this investigation, future studies testing how SUR2A-55 affects myocardial metabolism may lead to greater understanding of how mitoK_{ATP} affects both mitochondrial and cytoplasmic energy production.

4.2. Cardiomyocytes with increased expression of SUR2A-55 leads to cardioprotection

The location and significance of the SUR2-55 splice variant was originally presented by Ye et. al. [20] who described a SUR2-55 short-form based ATP-sensitive potassium channel that was insensitive to diazoxide and targeted to the mitochondria. $SUR2^{-/-}$ mice, which removed full length SUR2 but not SUR2A-55, displayed episodic vasospasm, sudden cardiac death, and enhanced insulin dependent glucose uptake [20, 23, 24]. The splice variant was formed through a nonconventional intraexonic splicing event within the 5^{th} and 30^{th} exons of the SUR2 mRNA. When subjected to IR injury, this $SUR2^{-/-}$ mouse was found to have reduced infarction compared to controls [20, 34]. In this current investigation we found that mice overexpressing the SUR2A-55 splice variant have improved tolerance to IR injury compared to controls. Unlike $SUR2^{-/-}$ mice, the $TG^{SUR2A-55}$ mice express the long form of SUR2 which is also found in mitochondria [20] and thus cardioprotection can occur with the expression of both splice variants. In addition, periodic vasospasm which is reported in the $SUR2^{-/-}$ mouse, is not expected in the $TG^{SUR2A-55}$ mouse and therefore does not explain the protected phenotype. We speculate from these studies that a switch from mitoK_{ATP} formed predominantly with the long-form SUR2 splice variant to the short-form splice variant channel can cause a cardioprotective phenotype. Whether or not a switch to SUR2A-55 dominated mitoK_{ATP} underlies cardioprotection in ischemic preconditioning requires further study. Therapies aimed at triggering a switch in SUR2 splice variant composition of mitoK_{ATP} may be an option for cardioprotective drugs in the future.

4.3. Overexpression of SUR2A-55 changes $\Delta\psi_m$ response to pharmacology and has implication for the regulation of mitoK_{ATP}

Mitochondria play a paramount role in cell death. During myocardial ischemia reperfusion injury, Ca^{2+} entry into the mitochondria ultimately leads to the mitochondrial transition pore (MPTP) opening and cell death [35, 36]. In our investigation, we found that mitochondria from $TG^{SUR2A-55}$ are more resistant to Ca^{2+} loading. In addition, we observed that the $\Delta\psi_m$ from $TG^{SUR2A-55}$ mitochondria are less sensitive

https://doi.org/10.1016/j.heliyon.2018.e00677

to ATP concentration and have less responsiveness to diazoxide. Interestingly, the percent difference in $\Delta\psi_m$ at low and high ATP concentrations in this report is similar to prior studies on the SUR2$^{-/-}$ mice [26] in which the SUR2A-55 isoform was preserved. While the electron transport chain and a number of channels in the mitochondria may be the reason for changes in $\Delta\psi_m$ [37], the change in sensitivity to ATP and diazoxide, as well as prior studies on SUR2A-55 make mitoK$_{ATP}$ the most likely target responsible for our observed data. However, direct measurements of mitoK$_{ATP}$ currents were not assessed. These data support prior work that SUR2A-55 promotes a mitoK$_{ATP}$ channel that is insentive to diaxoxide and ATP. The lack of ATP or diazoxide to change $\Delta\psi_m$ suggest a persistent potassium leak and constituently active mitoK$_{ATP}$ channel [22, 26].The mitochondrial membrane depolarization that ensues even in times of increased ATP, such as reperfusion, can result in lower mitochondrial calcium entry and reduced MPTP opening. Prior reports have suggested this as a mechanisms for protection from mitoK$_{ATP}$ activation and our data would continue to support this theory [38, 39, 40].

Further study in this area is challenging given the elusive nature of the mitoK$_{ATP}$ channel. However, recent data suggested that ROMK2 may be the pore forming unit of mitoK$_{ATP}$ [15]. Molecular reconstitution studies and gene deletion studies show that ROMK interacts with an ABC binding cassette to manifest native channel properties [41]. Additional studies have shown that ROMK2 binds to an another SUR2 splice variant, SUR2B, to form sulfonylurea sensitive K^+ channels that were not observed with ROMK1 or ROMK3. It is unknown if other splice variants of SUR can create native functional channels with ROMK. Further investigations studying interactions of ROMK2 and SUR2A splice variants may shed light on the molecular identity of mitoK$_{ATP}$. Our research suggests considerable plasticity of the mitoK$_{ATP}$ channel with different subunits affecting the channels response to pharmacology. This may also explain the elusive nature of the mitoK$_{ATP}$ channel and conjecture surrounding its existence.

While our current investigations describe the response of SUR2A-55 overexpression in mice, certain limitations exist. For practical reasons of scope, we restricted study to overexpression of the A isoform of SUR2. Prior studies have shown that both SUR2A-55 and SUR2B-55 isoforms exist [20, 21]. Therefore the SUR2B isoforms may also have physiologic significance and play a role in mitochondrial function. We concentrated on the SUR2A-55 isoform as our prior work showed qualitiatvely increased expression of SUR2A-55 over SUR2B-55 in mouse hearts [20]. In addition, due to the scope of our research, we restricted our study to male mice. While previous studies have shown targeting of the SUR2A-55 protein to mitochondria, we did not assess its location in TG$^{SUR2A-55}$ and did not measure potassium flux in mitochondria. However, our mitochondrial biophysical studies suggest a direct effect for SUR2A-55 on mitochondria.We also used a global ischemia *ex vivo* model for IR injury which has different physiologic stress than

https://doi.org/10.1016/j.heliyon.2018.e00677

a coronary ligation model and may not be as translational to human disease. In addition, while we report cardioprotection to IR injury and changes in mitonchondrial biophysical properties in $TG^{SUR2A-55}$ mice, there may be other cellular mechanisms including changes in sarcK_{ATP} activity that could be responsible for the cardioprotective response. Further studies on the role of SUR2A-55 in sarcK_{ATP} activity are needed.

5. Conclusion

In conclusion, elucidating pathways in cardioprotection may lead to improved clinical treatment of heart disease. While great advances have been made in the treatment of ischemic heart disease, it remains the leading cause for the development of heart failure [42, 43] and imposes a large burden on society [44]. In this research investigation, we showed that SUR2 splice variants offer an interesting area of further research to clarify mitochondrial function in ischemic heart disease. By altering the expression of SUR2 splice variants, different cardiac phenotypes arise. The overexpression of the SUR2A-55 splice variant leads to cardioprotection likely through a constitutively active mitoK_{ATP} channel. Further research to identify the components of the mitoK_{ATP} channel that enhance the cardioprotective phenotype should be considered using the $TG^{SUR2A-55}$ mouse.

Declarations

Author contribution statement

Mohun Ramratnam: Conceived and designed the experiments; Performed the experiments; Analyzed and interpreted the data; Contributed reagents, materials, analysis tools or data; Wrote the paper.

Barrett Kenny: Performed the experiments; Analyzed and interpreted the data; Contributed reagents, materials, analysis tools or data.

John W. Kyle: Conceived and designed the experiments; Performed the experiments; Analyzed and interpreted the data; Contributed reagents, materials, analysis tools or data.

Brandi Wiedmeyer: Performed the experiments; Analyzed and interpreted the data; Contributed reagents, materials, analysis tools or data; Wrote the paper.

Timothy A. Hacker: Contributed reagents, materials, analysis tools or data.

David Y. Barefield: Analyzed and interpreted the data.

Elizabeth M. McNally, Jonathan C. Makielski: Conceived and designed the experiments; Wrote the paper.

https://doi.org/10.1016/j.heliyon.2018.e00677

Funding statement

This work was supported by National Institutes of Health grant R01HL122109 (to EMM and JCM).

Competing interest statement

The authors declare no conflict of interest.

Additional information

Supplementary content related to this article has been published online at https://doi.org/10.1016/j.heliyon.2018.e00677.

Acknowledgements

We thank Katarzyna Borys for manuscript preparation and Emily Lacount for technical assistance with experiments. We thank Dr Nan Shi and Nitin Aggrawal for early assistance with the model.

References

[1] A. Noma, ATP-regulated K+ channels in cardiac muscle, Nature 305 (1983) 147−148. PMID: 6310409.

[2] M. Suzuki, et al., Role of sarcolemmal K(ATP) channels in cardioprotection against ischemia/reperfusion injury in mice, J. Clin. Invest. 109 (2002) 509−516.

[3] T. Sato, N. Sasaki, J. Seharaseyon, B. O'Rourke, E. Marban, Selective pharmacological agents implicate mitochondrial but not sarcolemmal K(ATP) channels in ischemic cardioprotection, Circulation 101 (2000) 2418−2423. PMID: 10821820.

[4] K.D. Garlid, et al., Cardioprotective effect of diazoxide and its interaction with mitochondrial ATP-sensitive K+ channels. Possible mechanism of cardioprotection, Circ. Res. 81 (1997) 1072−1082. PMID: 9400389.

[5] I. Inoue, H. Nagase, K. Kishi, T. Higuti, ATP-sensitive K+ channel in the mitochondrial inner membrane, Nature 352 (1991) 244−247.

[6] Z. Fan, J.C. Makielski, Intracellular H+ and Ca2+ modulation of trypsin-modified ATP-sensitive K+ channels in rabbit ventricular myocytes, Circ. Res. 72 (1993) 715−722. PMID: 8381726.

[7] H. Ardehali, B. O'Rourke, Mitochondrial K(ATP) channels in cell survival and death, J. Mol. Cell. Cardiol. 39 (2005) 7–16.

[8] G.C. Kane, X.K. Liu, S. Yamada, T.M. Olson, A. Terzic, Cardiac KATP channels in health and disease, J. Mol. Cell. Cardiol. 38 (2005) 937–943.

[9] M.N. Foster, W.A. Coetzee, KATP channels in the cardiovascular system, Physiol. Rev. 96 (2016) 177–252.

[10] N.Q. Shi, B. Ye, J.C. Makielski, Function and distribution of the SUR isoforms and splice variants, J. Mol. Cell. Cardiol. 39 (2005) 51–60.

[11] M. Yamada, et al., Sulphonylurea receptor 2B and Kir6.1 form a sulphonylurea-sensitive but ATP-insensitive K+ channel, J. Physiol. 499 (Pt 3) (1997) 715–720. PMID: 9130167.

[12] S. Seino, T. Miki, Physiological and pathophysiological roles of ATP-sensitive K+ channels, Prog. Biophys. Mol. Biol. 81 (2003) 133–176. PMID: 12565699.

[13] T.P. Flagg, D. Enkvetchakul, J.C. Koster, C.G. Nichols, Muscle KATP channels: recent insights to energy sensing and myoprotection, Physiol. Rev. 90 (2010) 799–829.

[14] A. Morrissey, et al., Immunolocalization of KATP channel subunits in mouse and rat cardiac myocytes and the coronary vasculature, BMC Physiol. 5 (2005) 1.

[15] D.B. Foster, et al., Mitochondrial ROMK channel is a molecular component of mitoK(ATP), Circ. Res. 111 (2012) 446–454.

[16] P. Bednarczyk, et al., Evidence for a mitochondrial ATP-regulated potassium channel in human dermal fibroblasts, Biochim. Biophys. Acta 1859 (2018) 309–318.

[17] R. Bajgar, S. Seetharaman, A.J. Kowaltowski, K.D. Garlid, P. Paucek, Identification and properties of a novel intracellular (mitochondrial) ATP-sensitive potassium channel in brain, J. Biol. Chem. 276 (2001) 33369–33374.

[18] P. Paucek, et al., Reconstitution and partial purification of the glibenclamide-sensitive, ATP-dependent K+ channel from rat liver and beef heart mitochondria, J. Biol. Chem. 267 (1992) 26062–26069. PMID: 1464617.

[19] M. Suzuki, et al., Kir6.1: a possible subunit of ATP-sensitive K+ channels in mitochondria, Biochem. Biophys. Res. Commun. 241 (1997) 693–697.

[20] B. Ye, et al., Molecular identification and functional characterization of a mitochondrial sulfonylurea receptor 2 splice variant generated by intraexonic splicing, Circ. Res. 105 (2009) 1083–1093.

https://doi.org/10.1016/j.heliyon.2018.e00677

[21] T. Ballantyne, et al., Testosterone protects female embryonic heart H9c2 cells against severe metabolic stress by activating estrogen receptors and up-regulating IES SUR2B, Int. J. Biochem. Cell Biol. 45 (2013) 283−291.

[22] N.T. Aggarwal, N.Q. Shi, J.C. Makielski, ATP-sensitive potassium currents from channels formed by Kir6 and a modified cardiac mitochondrial SUR2 variant, Channels 7 (2013) 493−502.

[23] W.A. Chutkow, et al., Episodic coronary artery vasospasm and hypertension develop in the absence of Sur2 K(ATP) channels, J. Clin. Invest. 110 (2002) 203−208.

[24] W.A. Chutkow, et al., Disruption of Sur2-containing K(ATP) channels enhances insulin-stimulated glucose uptake in skeletal muscle, Proc. Natl. Acad. Sci. U.S.A. 98 (2001) 11760−11764.

[25] R. Kakkar, et al., Spontaneous coronary vasospasm in KATP mutant mice arises from a smooth muscle-extrinsic process, Circ. Res. 98 (2006) 682−689.

[26] N.T. Aggarwal, et al., The mitochondrial bioenergetic phenotype for protection from cardiac ischemia in SUR2 mutant mice, Am. J. Physiol. Heart Circ. Physiol. 299 (2010) H1884−H1890.

[27] J.P. Fahrenbach, et al., Abcc9 is required for the transition to oxidative metabolism in the newborn heart, FASEB J. 28 (2014) 2804−2815.

[28] A. Subramaniam, et al., Tissue-specific regulation of the alpha-myosin heavy chain gene promoter in transgenic mice, J. Biol. Chem. 266 (1991) 24613−24620. PMID: 1722208.

[29] B. Ostadal, P. Ostadal, Sex-based differences in cardiac ischaemic injury and protection: therapeutic implications, Br. J. Pharmacol. 171 (2014) 541−554.

[30] E. Murphy, C. Steenbergen, Gender-based differences in mechanisms of protection in myocardial ischemia-reperfusion injury, Cardiovasc. Res. 75 (2007) 478−486.

[31] J.L. Pu, et al., Cardiac sulfonylurea receptor short form-based channels confer a glibenclamide-insensitive KATP activity, J. Mol. Cell. Cardiol. 44 (2008) 188−200.

[32] D. Pravdic, et al., Anesthetic-induced preconditioning delays opening of mitochondrial permeability transition pore via protein Kinase C-epsilon-mediated pathway, Anesthesiology 111 (2009) 267−274.

[33] M. Ljubkovic, et al., Isoflurane preconditioning uncouples mitochondria and protects against hypoxia-reoxygenation, Am. J. Physiol. Cell Physiol. 292 (2007) C1583−C1590.

https://doi.org/10.1016/j.heliyon.2018.e00677

[34] D. Stoller, et al., Mice lacking sulfonylurea receptor 2 (SUR2) ATP-sensitive potassium channels are resistant to acute cardiovascular stress, J. Mol. Cell. Cardiol. 43 (2007) 445−454.

[35] A.P. Halestrap, What is the mitochondrial permeability transition pore? J. Mol. Cell. Cardiol. 46 (2009) 821−831.

[36] G. Heusch, Molecular basis of cardioprotection: signal transduction in ischemic pre-, post-, and remote conditioning, Circ. Res. 116 (2015) 674−699.

[37] B. O'Rourke, Mitochondrial ion channels, Annu. Rev. Physiol. 69 (2007) 19−49.

[38] P. Korge, H.M. Honda, J.N. Weiss, Protection of cardiac mitochondria by diazoxide and protein kinase C: implications for ischemic preconditioning, Proc. Natl. Acad. Sci. U.S.A. 99 (2002) 3312−3317.

[39] M. Murata, M. Akao, B. O'Rourke, E. Marban, Mitochondrial ATP-sensitive potassium channels attenuate matrix Ca(2+) overload during simulated ischemia and reperfusion: possible mechanism of cardioprotection, Circ. Res. 89 (2001) 891−898. PMID: 11701616.

[40] L. Wang, et al., Preconditioning limits mitochondrial Ca(2+) during ischemia in rat hearts: role of K(ATP) channels, Am. J. Physiol. Heart Circ. Physiol. 280 (2001) H2321−H2328.

[41] P.A. Welling, K. Ho, A comprehensive guide to the ROMK potassium channel: form and function in health and disease, Am. J. Physiol. Ren. Physiol. 297 (2009) F849−F863.

[42] Y. Gerber, et al., Mortality associated with heart failure after myocardial infarction: a contemporary community perspective, Circulation. Heart Failure 9 (2016), e002460.

[43] R.S. Velagaleti, et al., Long-term trends in the incidence of heart failure after myocardial infarction, Circulation 118 (2008) 2057−2062.

[44] Z. Zhao, Y. Zhu, Y. Fang, W. Ye, P. McCollam, Healthcare resource utilization and costs in working-age patients with high-risk atherosclerotic cardiovascular disease: findings from a multi-employer claims database, J. Med. Econ. 18 (2015) 655−665.

https://doi.org/10.1016/j.heliyon.2018.e00677